Military Technical College
Kobry El-Kobbah,
Cairo, Egypt

14th International Conference on Applied Mechanics and Mechanical Engineering
AMME-14

Analysis of an Adaptive Magnetorheological Sandwich Beam Structure Based on Finite Element and Spectral Element Formulations

By

Peter L. Bishay* Mohammad Tawfik** Hani M. Negm***

Abstract:

The Magnetorheological fluid, as one of the smart materials, is the focus of many researches running nowadays and is getting to replace many materials in several engineering applications. This fluid is characterized by its ability to change from liquid into semi-solid gel in few milliseconds as a result of applying magnetic field.
This paper deals with a magnetorheological fluid embedded in an Aluminum sandwich beam to give the whole sandwich structure relevant controllability of various parameters such as natural frequencies, vibration amplitudes, and damping factors.
This paper presents Finite Element formulation of the MR sandwich beam, and uses the finite element model to solve for various beam boundary conditions, various magnetic field levels and configurations. The paper also compares the finite element results with published analytical and the experimental results.
Finally, the paper checks the suitability of the spectral element method in dealing with the MR sandwich beam, and compares the spectral results with the finite element results.

Keywords:

Spectral element, Finite element, Magnetorheological fluid, Sandwich beam

---

* Teaching Assistant, Aerospace Engineering Department, Cairo University
** Assistant Professor, Aerospace Engineering Department, Cairo University
*** Professor Emeritus, Aerospace Engineering Department, Cairo University

1. Introduction:

Magnetorheological (MR) fluids belong to the class of controllable fluids. The essential characteristic of MR fluids is their ability to reversibly change from free-flowing, linear viscous liquids to semi-solids having controllable yield strength in milliseconds when exposed to a magnetic field. This yield stress increases with the applied magnetic field. This feature provides simple, quiet, rapid response interfaces between electronic controls and mechanical systems [1].
These fluids are suspensions of micron-sized magnetic particles in an appropriate carrier liquid. There are different types of liquids which can be used as the carrier fluid i.e. hydrocarbon oils, mineral oils and silicon oils. Normally, MR fluids are free flowing liquids having a consistency similar to that of motor oil. However, in the presence of an applied magnetic field, the iron particles acquire a dipole moment aligned with the external field which causes particles to form linear chains parallel to the field. This phenomenon can solidify the suspended iron particles and restrict the fluid movement.

1.1 Applications of MR fluids in adaptive sandwich beam structures

Typically, MR adaptive structures are achieved by having MR material layers placed in solid metal or composite layers. The dynamic response of the structure can be varied when different levels of magnetic field are applied over the MR layer, which in turn produce structures with variable stiffness and damping properties. These variations in the rheological properties of MR materials are fast (a few milliseconds) and reversible, in response to variations in applied magnetic field, and can manipulate the dynamic vibration responses of the composite quickly. By controlling the applied magnetic field, the vibration of adaptive structures can be minimized for a broad range of external excitation frequencies.

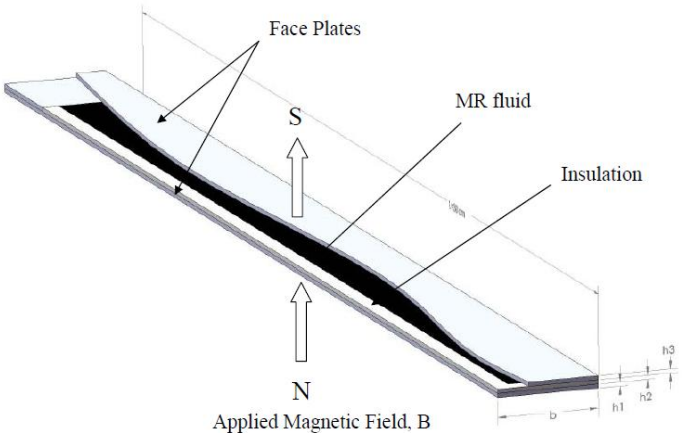

***Figure (1):** Three-layered adaptive beam configuration with MR material situated in the middle layer*

Yalcintas [2] turned to the MR sandwich beam problem after making a performance comparison between ER and MR sandwich beams. From that study it was observed that both ER and MR adaptive structures show variations in their vibration responses when subjected to electric field and magnetic field respectively. These variations were mainly a decrease in vibration amplitudes and loss factors, and an increase in the natural frequency when the electric/magnetic field is increased. However, variations were more significant for MR adaptive structures than for the ER adaptive structures.
Yalcintas and Dai [3], followed by Sun et al. [4], developed a theoretical model for the MR sandwich beam and solved it for the case of Simply Supported beams to predict its vibration response. Since the MR materials have higher stiffness values, the shear stresses experienced remain in the pre-yield regime. Therefore, the energy model considered in Yalcintas' study was based on the pre-yield rheological properties of MR materials.
Spectral analysis has been used for the approximate solution of different types of structural vibration problems. Doyle [5] used exponential interpolation functions with a wave length parameter that changes with the frequency for the bars and beams' finite element models that suit the nature of a structural dynamics problem.
Mahapatra et al.[6] presented a spectral finite element model for the study of composite beams. Wang and Wereley [7] presented a formulation for the application of spectral element analysis to a sandwich beam with a viscoelastic core. The spectral element method provided much higher accuracy with a smaller number of elements as compared to the traditional finite element method.
In this paper, the modeling of a Magnetorhelolgical (MR) sandwich beam structure using the spectral element and the higher order finite element methods in structural analysis will be presented for the first time.

1.2 MR material rheological properties

According to MR rheological studies, the shear stress–shear strain relation is analyzed in two regimes as pre-yield and post-yield regimes. These behaviors are illustrated in Figure (*2*).

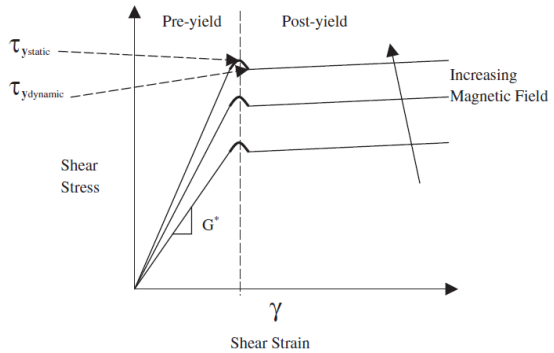

***Figure (2):** Shear stress –shear strain relationship of MR materials*

In the earlier studies, the MR pre-yield regime was modeled by a linear viscoelastic model, and the post-yield regime was modeled by the Bingham plastic model. Li *et al* [8] verified, through step-strain experiments, that the MR pre-yield behavior is linearly viscoelastic up to 0.1% shear strain, and nonlinear above the 0.1% shear strain.
In the three-layered sandwich beam configuration, the MR materials experience shear stress and shear strain that is confined in the pre-yield regime. Yalcintas [9] determined that the shear strain experienced by the MR layer is then below 0.1%. Therefore, the linear viscoelastic theory is valid for MR adaptive structures.

2. ***Finite Element and Spectral Element Modeling of the Three-Layer sandwich beam:***

In the following analysis we shall use Mead and Markus (MM) assumptions:

- The transverse displacement (w) is the same for all the three layers.
- Rotary inertia and shear deformations in the upper and lower elastic layer beams are negligible.
- The Core layer has negligible bending stiffness and is subjected only to shear given by $\gamma = \frac{\partial w}{\partial x} + \frac{\partial u}{\partial z}$
- Linear theories of elasticity and viscoelasticity are valid.
- No slip occurs between the layers, and there is perfect continuity at the interface.
- All displacements are small.

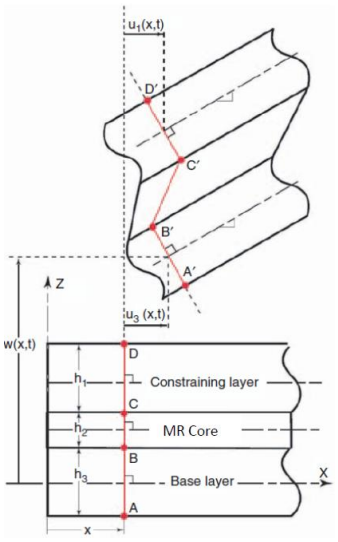

Figure (3): *The undeformed (dashed line) and the deformed (Solid line) configurations of a three-layer sandwich beam under lateral loading*

The beam deformations are shown in Figure (*3*). A fundamental assumption of the approach is that line B-C in the core layer remains straight after deformation, as shown

by line B'-C' in Figure (*3*). This, in effect, defines the axial deformation of any material position (*x*) inside the core as a linear interpolation of the displacements u_1' and u_3' on the surfaces of the face-sheets.

It can be proved that the axial displacement and the shear strain of the MR layer are given by[10]:

$$u_2 = \frac{u_1 + u_3}{2} + \frac{h_1 - h_3}{4} + \frac{\partial w}{\partial x} \quad (1)$$

$$\gamma_{zx} = \frac{u_3 - u_1}{h_2} + \frac{d}{h_2}\frac{\partial w}{\partial x} \quad (2)$$

where $d = \frac{h_1}{2} + h_2 + \frac{h_3}{2}$ is the distance between the reference lines of the undeformed face-sheets.

Since the beam is assumed not subjected to longitudinal loading, the resultant of the longitudinal normal force must vanish, i.e.,

$$E_1 A_1 \frac{\partial u_1}{\partial x} + E_3 A_3 \frac{\partial u_3}{\partial x} = 0 \quad (3)$$

Integrating with respect to *x* and expressing u_3 in terms of u_1, we have

$$u_3 = -e u_1, \qquad \text{where } e = \frac{E_1 A_1}{E_3 A_3} \quad (4)$$

Hence,

$$u_2 = \frac{(1-e)}{2} u_1 + \frac{(h_3 - h_1)}{4}\frac{\partial w}{\partial x} \quad (5)$$

and $$\gamma_{zx} = -\frac{(1+e)}{h_2} u_1 + \frac{d}{h_2}\left(\frac{\partial w}{\partial x}\right) \quad (6)$$

For simplicity, we will use "u" instead of "u_1".

2.1 ***Development of the equations of motion:***

The equations of motion in this investigation are developed using *Hamilton's principle*:

$$\delta\left(\int_{t1}^{t2}(T - U - V)dt\right) = 0 \quad (7)$$

where *T* is the kinetic energy, *U* is the strain energy, and *V* is the work done by external forces.

By taking the first variation, then integrating by parts with respect to time (t_1 and t_2 are arbitrary), we get the weak form of Hamilton's principle, which is used for deriving the finite element equations of the system.

For the core layer, we may write:

$$U_2 = \frac{1}{2} G_2 A_2 \int_0^L \gamma_{zx}^2 dx \quad (8)$$

$$T_2 = \frac{1}{2}\rho_2 A_2 \int_0^L \left(\frac{\partial u_2}{\partial t}\right)^2 dx + \frac{1}{2}\rho_2 A_2 \int_0^L \left(\frac{\partial w}{\partial t}\right)^2 dx \quad (9)$$

where G_2 is the complex shear modulus and γ_{zx} is the shear strain. From the above, we may write:

$$U_2 = \frac{1}{2} G_2 A_2 \int_0^L \left(- \frac{(1+e)}{h_2} u + \frac{d}{h_2} \left(\frac{\partial w}{\partial x} \right) \right)^2 dx \quad (10)$$

$$T_2 = \frac{1}{2} \rho_2 A_2 \int_0^L \left(\frac{\partial}{\partial t} \left(\frac{(1-e)}{2} u + \frac{(h_3 - h_1)}{4} \frac{\partial w}{\partial x} \right) \right)^2 dx + \frac{1}{2} \rho_2 A_2 \int_0^L \left(\frac{\partial w}{\partial t} \right)^2 dx \quad (11)$$

Using this, we may write the total energy as:

$$U = \frac{1}{2} (E_1 A_1 + e^2 E_3 A_3) \int_0^L \left(\frac{\partial u}{\partial x} \right)^2 dx + \frac{1}{2} (E_1 I_1 + E_3 I_3) \int_0^L \left(\frac{\partial^2 w}{\partial x^2} \right)^2 dx + \frac{1}{2} G_2 A_2 \int_0^L [- \frac{(1+e)}{h_2} u + \frac{d}{h_2} (\frac{\partial w}{\partial x})]^2 dx \quad (12)$$

$$T = \frac{1}{2} (\rho_1 A_1 + e^2 \rho_3 A_3) \int_0^L \left(\frac{\partial u}{\partial t} \right)^2 dx + \frac{1}{2} (\rho_1 A_1 + \rho_2 A_2 + \rho_3 A_3) \int_0^L \left(\frac{\partial w}{\partial t} \right)^2 dx + \frac{1}{2} \rho_2 A_2 \int_0^L \frac{\partial}{\partial t} [\frac{(1-e)}{2} u + \frac{(h_3 - h_1)}{4} \frac{\partial w}{\partial x}]^2 dx \quad (13)$$

*2.2 **Finite Element Shape Functions***

In this paper, different beam models are used with different numbers of nodes. Also, the interpolation functions used are regular polynomials and exponential functions for the spectral element.

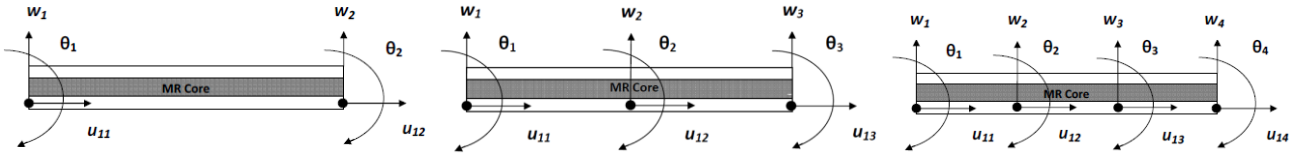

***Figure (4):** The proposed 2-node, 3-node, and 4-node sandwich beam elements with three degrees-of-freedom per node*

The polynomial shape function for the longitudinal displacement $u(x)$ and the transverse deflection $w(x)$ are:

$$u(x) = \sum_0^n a_i x^i \qquad 0 \le x \le L \quad (14)$$

$$w(x) = \sum_0^{2n} c_i x^i \qquad 0 \le x \le L \quad (15)$$

where n is the number of nodes in the element.

For the spectral element model, the longitudinal displacement $u(x)$ and the transverse displacement $w(x)$ shape functions are:

$$u(x) = a_o e^{ik_u x} + a_1 e^{-ik_u x} \qquad 0 \le x \le L \quad (16)$$

$$w(x) = c_o e^{k_w x} + c_1 e^{-k_w x} + c_2 e^{ik_w x} + c_3 e^{-ik_w x} \qquad 0 \le x \le L \quad (17)$$

where $k_u = \frac{\omega}{C}$ and $k_w = \left(\frac{\omega^2 \rho h}{D} \right)^{\frac{1}{4}}$ are the wave numbers, ω is the frequency, $C = \sqrt{\frac{E}{\rho}}$ is the longitudinal wave speed and D is the flexural rigidity of the beam. For the case of

Sandwich beam $C = \sqrt{\frac{E_1}{\rho_1}}$, $D = E_1 I_1 + E_3 I_3$ and $k_w = \left(\frac{\omega^2(\rho_1 h_1 + \rho_2 h_2 + \rho_3 h_3)}{D}\right)^{\frac{1}{4}}$

2.3 ***Finite element model***

According to the normal procedure of the finite element method that could be found in any finite element textbook, we can rewrite the shape functions in the form:

$u(x) = \lfloor N_u \rfloor \{\delta_u\}$ (18)

$w(x) = \lfloor N_w \rfloor \{\delta_w\}$ (19)

where $\{\delta_u\} = \{u_1 \quad u_2 \quad \dots \quad u_n\}^T$

and $\{\delta_w\} = \{w_1 \quad \theta_1 \quad w_2 \quad \theta_2 \quad \dots \quad w_n \quad \theta_n\}^T$

Thus the element matrices may be written as:

$U = \frac{1}{2} \{\delta\}^T [K] \{\delta\}$ (20)

where $[K] = [K^u] + [K^w] + [K^\gamma]$,

$[K^u] = (E_1 A_1 + e^2 E_3 A_3) \int_0^L \{N_{u_x}\} \left\lfloor N_{u_x} \right\rfloor dx,$

$[K^w] = (E_1 I_1 + E_3 I_3) \int_0^L \{N_{w_{xx}}\} \left\lfloor N_{w_{xx}} \right\rfloor dx,$

$[K^\gamma] = G_2 A_2 \int_0^L \{N_\gamma\} \left\lfloor N_\gamma \right\rfloor \, dx$

$T = \frac{1}{2} \{\delta\}^T [M] \{\delta\}$ (21)

where $[M] = [M^u] + [M^w] + [M^v]$

$[M^u] = (\rho_1 A_1 + e^2 \rho_3 A_3) \int_0^L \{N_u\} \lfloor N_u \rfloor \, dx$

$[M^w] = (\rho_1 A_1 + \rho_2 A_2 + \rho_3 A_3) \int_0^L \{N_w\} \lfloor N_w \rfloor \, dx,$

$[M^v] = \rho_2 A_2 \int_0^L \{N_v\} \lfloor N_v \rfloor \, dx$

Finally, the element equation of motion becomes:

$[M]\{\ddot{U}\} + [K]\{U\} = \{F\}$ (22)

$\{F\}$ is the external load vector, and will be set to zero during the frequency response analysis.

A general MATLAB code for any-order element was developed to calculate the global mass and stiffness matrices for the MR sandwich beam, and hence calculate the natural frequencies and the loss factors for the MR sandwich beam for various beam boundary conditions. Another MATLAB code for the Spectral element was developed too.

3. ***Numerical Validation***

The above developed mass and stiffness matrices for the sandwich beam elements with MRF core layer were used to calculate the natural frequencies and loss factors of an example beam Simply Supported from both ends with main dimensions and

characteristics as in the paper of Yalcintas [3] for the sake of comparison with the analytical model and results found in this reference paper.
The main dimensions and properties of the MRF sandwich beam in [3] are:
Beam length: L = 393.7 mm, Beam width: b = 25.4 mm,
Elastic Layers properties: Material: Aluminum,
Elastic modulus: E = 70 GPa, Density: $\rho = 2700$ Kg/m^3,
Thickness: $h_1 = h_3 = 0.7353$ mm
MR layer properties: $G^* = G'(B) + G''(B)\,i$
where: $G'(B) = 3.11 * 10^{-7}\,B^2 + 3.56 * 10^{-4}\,B + 5.78 * 10^{-1}$,
$G''(B) = 3.47 * 10^{-9}\,B^2 + 3.85 * 10^{-6}\,B + 6.31 * 10^{-3}$, (for Sun's model[4])
Or, $G^*(B) = (1.25 \times 10^3 + i1.375 \times 10^1)B$.
The value of G* with no applied magnetic field was assumed as:
$G^*(0) = (0.6125 + i0.0067375)$ MPa (for Yalcintas' model [3]).
where B (Oersted) is the value of magnetic induction.
Density: $\rho = 3500$ Kg/m^3, Thickness: $h_2 = 0.7353$ mm

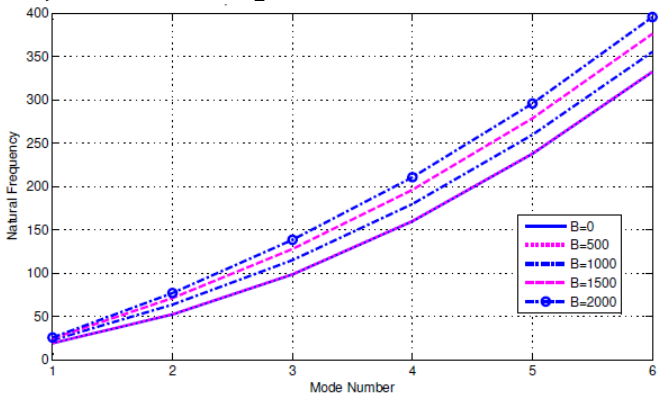

Figure (5): Effect of magnetic field on the natural frequencies of the MR sandwich beam for various Mode numbers

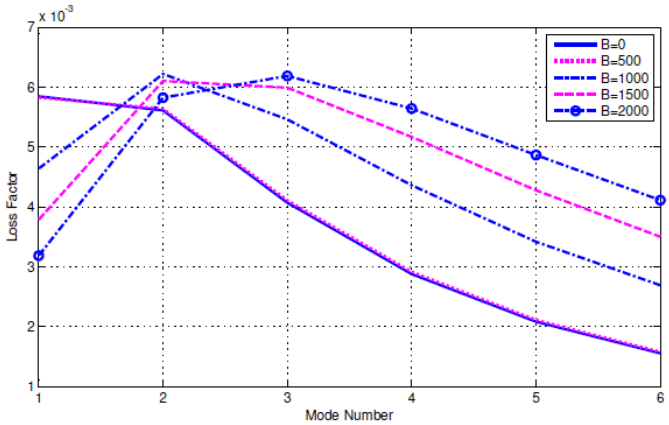

Figure (6): Effect of magnetic field on the loss factors of the MR sandwich beam for various Mode numbers

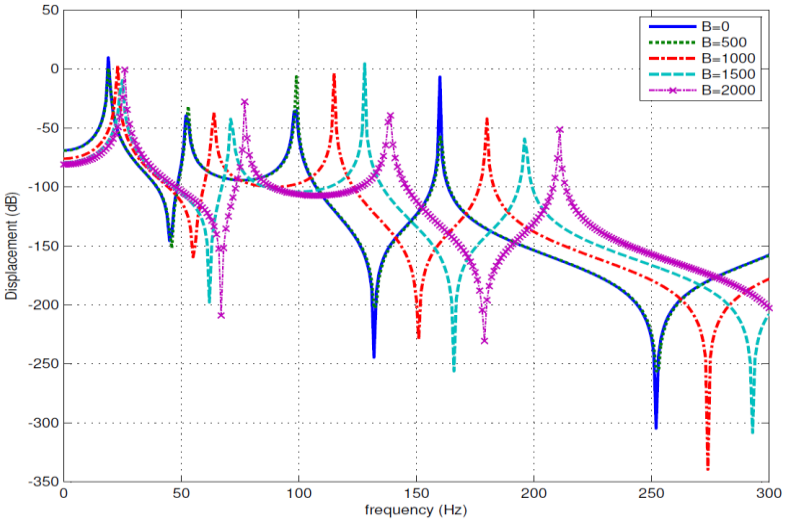

Figure (7): Effect of magnetic field on the Frequency response of the SS-SS MR sandwich beam

Figure (5) and Figure (6) show the effect of the magnetic field on the natural frequencies and loss factors of the SS-SS beam respectively up to the sixth mode. As can be seen from the figures, the natural frequencies shift to higher frequencies as the applied magnetic field increases. The loss factor decreases at the first mode and increases at higher modes as the magnetic field strength increases.

Figure 7 shows the effect of the magnetic field on the vibration amplitude of the MR sandwich beam. As the magnetic field strength increases, the vibration amplitude of each mode decreases, and the natural frequencies shift to higher frequencies. These variations are observed more significantly at higher frequencies. The actuation location is 218.4 mm from the left side of the beam, while the sensing location is at a point 78.7mm from the right side of the beam.

This type of response of MR adaptive beams is a strong evidence of the control capabilities of MR materials in adaptive structures.

These results were computed using 5 elements and then using 10 elements for the two-node, three-node and four-node elements' models in addition to the spectral element model. The results validate the correctness of the equations, matrices and computer codes of the suggested MR sandwich beam finite element and spectral element models. The results also show that the four-node element model gives very accurate results for natural frequencies and loss factors of the MR sandwich beam with error less than 1% with a smaller number of elements (3-5 elements). The three-node element model follows in accuracy, and then the two-node element model; which could require 10-15 elements to give accurate results with error less than 1%. The spectral element model in the sandwich beam application unexpectedly gave accuracy slightly more than that of the 2-node FE, but less than that of the higher order FE models.

4. ***Applications of the FEM and SEM on the MR sandwich beams with several Boundary condition types:***

The presence of the Finite Element model or the Spectral Element model for the MR sandwich beam made it possible and easy to consider other beam boundary conditions beside the Simply Supported beam which was the only available case for the analytical model developed previously by Yalcintas [3] and Sun [4]. The presence of the Finite Element model or the Spectral Element model made it possible to activate any portion of the MR sandwich beam with magnetic field.
A MATLAB code has been developed to calculate the natural frequencies and loss factors for any-order-FE model or SE model for four kinds of MR sandwich beam boundary conditions which are: SS- SS, Fixed- Free, Fixed-SS, and Fixed- Fixed.
Application (1), given below, presents the natural frequencies and loss factors of the MR sandwich beam with several boundary conditions.
Application (2) deals with certain effective portions of SS-SS and Fixed-Fixed beams.
The MR sandwich beam dimensions and properties used in these applications are similar to found in Sun's paper [4].

Application (1):
In this application we calculate the natural frequencies and loss factors for the first five modes of several kinds of beam boundary conditions at different magnetic field levels. These results can't all be obtained using the analytical model derived in the papers of Yalcintas [3] and Sun [4]. For the sake of high accuracy, we used 20 elements of the three-node type.

Table (1): *Numerical results of the first three natural frequencies and loss factors of the MR sandwich beam with several kinds of boundary conditions at various magnetic field levels*

B.C. type	Mag. Field (Oe)	Natural Frequencies (Hz)			Loss Factor		
		Mode 1	Mode 2	Mode 3	Mode 1	Mode 2	Mode 3
SS-SS	0	20.9932	59.1363	116.6269	0.0062	0.0044	0.0027
	1000	25.9232	70.7952	131.9057	0.0057	0.0058	0.0043
	2000	30.54	86.1789	155.1905	0.0044	0.0062	0.0057
Fixed-Free	0	9.7745	38.5946	87.5442	0.0047	0.0046	0.0036
	1000	11.3189	45.8463	101.5695	0.0036	0.0051	0.0048
	2000	12.4823	54.2412	120.3411	0.0025	0.0052	0.0055
Fixed-SS	0	26.2954	69.564	132.7657	0.0052	0.0035	0.0022

	1000	32.0094	80.8011	147.2353	0.0059	0.005	0.0037
	2000	38.6297	96.5068	169.9328	0.0056	0.0059	0.0051
Fixed-Fixed	0	33.1945	81.4439	150.4351	0.0042	0.0028	0.0018
	1000	39.4622	91.9943	164.0862	0.0055	0.0042	0.0032
	2000	47.6956	107.5344	186.0359	0.006	0.0054	0.0046

Table (1) presents the values of the first three natural frequencies and loss factors for various MR sandwich beam boundary conditions at several magnetic field levels.
It is clear from the previous table that the effect of the magnetic field on the natural frequencies of the MR sandwich beam becomes more significant as the boundaries of the beam become more rigid i.e. the effect on the Fixed-Fixed natural frequencies is more than that on the Fixed-SS, Fixed-Free, and SS-SS natural frequencies. It is also clear that the effect of the magnetic field on the natural frequencies of the MR sandwich beam is more significant at higher modes.

Application (2):

From the above equations, it is clear that the shear strain of the MR layer depends on two factors: the relative axial displacement between the upper and lower layers, and the slope of the transverse displacement. Hence, for each beam boundary condition, each mode shape has some portions of the beam span that have more curvature than other portions. If these portions only are activated with the magnetic field, they will give almost the same targeted natural frequency as that of the totally activated MR sandwich beam. To illustrate this, we use a SS-SS MR sandwich beam made up of 30 elements. For the sake of accuracy the elements' model will be of the three-node type. The applied magnetic field on the beam is 2000 Oe. Targeting the first three natural frequencies, we will use three activation configurations as shown in Figure (8).

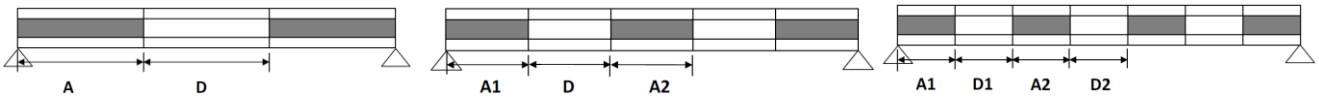

Figure (8): *The proposed activation configurations to target the first three modes of the SS-SS MR sandwich beam*

Table (2), Table (3) and Table (4) compares the natural frequencies of the fully activated and fully deactivated beams with the three proposed activation configurations for the SS-SS MR sandwich beam with several lengths of the activated portions. In this table, "A" refers to the activated length, while "D" refers to the deactivated length. Note that the activation pattern is symmetrical about the beam mid-span.

***Table (2):** Comparison of the first activation configuration with its different cases with the fully activated SS-SS MR sandwich beam*

				Mode 1 (Hz)	% from fully activated 1st natural freq.	Mode 2 (Hz)	Mode 3 (Hz)
Fully Activated				30.54		86.1789	155.1902
Case	A	D	% Active				
1	0.33L	0.33L	66 %	30.1419	98.70 %	69.8046	141.693
2	0.3L	0.4L	60 %	29.8181	97.64 %	68.2308	136.3095
3	0.27L	0.46L	54 %	29.3594	96.13 %	67.3487	131.9837
4	0.23L	0.54L	46 %	28.761	94.17 %	66.9819	129.1804
5	0.2L	0.6L	40 %	28.0326	91.79 %	66.9116	127.8563
Fully Deactivated				20.9932		59.1363	116.6269

It can be seen from Table (2) that with deactivation of almost half the beam length, the fundamental natural frequency is decreased by only 5% from the case of the fully activated MR sandwich beam (case 3 or 4).
Note that even in the first case where the deactivated portion is only one third of the total beam length and where the fundamental natural frequency is 98.7 % from that of the fully activated one, the second natural frequency of this case is far from that of the fully activated one. This is because the proposed configuration is targeting the first mode only.

***Table (3):** Comparison of the second activation configuration with its different cases with the fully activated SS-SS MR sandwich beam*

					Mode 1 (Hz)	Mode 2 (Hz)	% from fully activated 2nd natural freq.	Mode 3 (Hz)
Fully Activated					30.54	86.1789		155.1902
Case	A1	D	A2	% Active				
1	0.13L	0.2L	0.33L	60 %	27.1545	83.7372	97.17 %	141.7568
2	0.17L	0.2L	0.27L	60 %	27.7025	83.7372	97.17 %	136.5902
3	0.13L	0.23L	0.27L	53 %	26.7895	82.7023	96 %	136.536
4	0.2L	0.2L	0.2L	60 %	28.2683	81.8466	95 %	132.5573
Fully Deactivated					20.9932	59.1363		116.6269

It can be seen from Table (3) that with deactivation of almost 40% of the beam length, the second natural frequency is decreased by only 2.8% from the case of the fully activated MR sandwich beam (case 1 or 2), and with deactivation of almost 47% of the beam length, the second natural frequency is decreased by only 4% from the case of the fully activated MR sandwich beam (case 3).
Note that from the four cases of this configuration, the fourth case was the worst with respect to the second natural frequency, but it is the best with respect to the fundamental frequency, this is because this case is similar to the fifth case in the first configuration

which was targeting the fundamental natural frequency with 0.2L activated portion near each SS end.
Note also that even in the first case where the deactivated portion is only 40% of the total beam length and where the second natural frequency is 97.17 % from that of the fully activated one, the third natural frequency of this case is far from that of the fully activated one. This is because the proposed configuration is targeting the second mode only.

***Table (4):** Comparison of the third activation configuration with its different cases with the fully activated SS-SS MR sandwich beam*

						Mode 1	Mode 2	Mode 3	% from fully activated 2nd natural freq.
Fully Activated						30.54	86.1789	155.1902	
Case	A1	D1	A2	D2	% Active				
1	0.13L	0.07L	0.23L	0.13L	73 %	28.7358	81.321	153.768	99 %
2	0.13L	0.1L	0.2L	0.13L	67 %	28.7174	77.7586	152.8231	98.4 %
3	0.13L	0.13L	0.2L	0.07L	67 %	28.1426	81.2749	151.1431	97.4 %
4	0.13L	0.13L	0.17L	0.13L	60 %	28.1223	77.7311	150.2472	96.8 %
5	0.13L	0.17L	0.13L	0.13L	53 %	27.584	77.6481	146.0131	94.08 %
Fully Deactivated						20.9932	59.1363	116.6269	

It can be seen from Table (4) that with deactivation of almost 40% of the beam length, the third natural frequency is decreased by only 3.2% from the case of the fully activated MR sandwich beam (case 4), and with deactivation of almost 46% of the beam length, the third natural frequency is decreased by only 6% (case 5).
As a final conclusion, with only 60% activated beam span we can target any mode by placing the activated portions in the proper places to get the effect of the fully activated MR sandwich beam at this mode.

5. Conclusion

In this paper we have developed a spectral and a higher order finite element models for the MR sandwich beam. The proposed models were used to perform modal analysis and calculate frequencies and loss factors of a MR sandwich beam, and the results were compared with the analytical model results published previously. It was shown that the 4-node element model gives the highest accuracy with a small number of elements.
Then we used the developed models in two applications, the first was investigating the dynamic characteristics of different MR sandwich beam boundary conditions that were unavailable in the previous analytical models. The second was investigating the critical portions to be activated on the beam span to get the natural frequencies of the fully activated MR sandwich beam. In these applications we have proposed several activation configurations in targeting the first, second and third modes of a SS-SS sandwich beam.

We have shown that we can get the same effect of the fully activated MR sandwich beam by activating only 60 % of the beam span at the proper portions regarding the targeted mode and the required boundary conditions.

References

[1] G.Yang, 2001, "Large-Scale Magnetorheological Fluid Damper for Vibration Mitigation: Modeling, Testing and Control," *Ph.D dissertation*, *University of Notre Dame*, 2001. http://cee.uiuc.edu/sstl/gyang2/ch2.pdf.

[2] Melek Yalcintas and Heming Dai, 1999, "Magnetorheological and Electrorheological Materials in Adaptive Structures and their Performance Comparison", *Smart Mater. Struct.* 8 (1999) 560–573.

[3] Melek Yalcintas and Heming Dai, 2004, "Vibration Suppression Capabilities of Magnetorheological Materials Based Adaptive Structures", *Smart Mater. Struct.* 13 (2004) 1–11

[4] Qing Sun, Jin-Xiong Zhou, Ling Zhang, 2003, "An Adaptive Beam Model and Dynamic Characteristics of Magnetorheological Materials", *Journal of Sound and Vibration* 261 (2003) 465–481

[5] Doyle, J. F., 1997, "Wave Propagation in Structures: Spectral Analysis Using Fast Discrete Fourier Transforms," *Mechanical Engineering Series*, 2nd ed., *Springer-Verlag*.

[6] Mahapatra, D. R., Gopalakrishnan, S., and Sankar, T. S., 2000, "Spectral-Element-Based Solutions for Wave Propagation Analysis of Multiply Connected Unsymmetrical Laminated Composite Beams," *Journal of Sound and Vibration*, Vol. 237, No. 5, 2000, pp. 819-836.

[7] Wang, G. and Wereley, N. M., 1999, "Spectral Finite Element Analysis of Sandwich Beams with Passive Constrained Layer Damping," *40th AIAA/ASME/ASCE/AHS/ASC Structures, Structural Dynamics, and Materials Conference and Exhibit*, American Institute of Aeronautics and Astronautics, 1999, p. 2681-2694.

[8] Li WH, Du H, Chen G, Yeo S H and Guo N Q, 2002, "Nonlinear Rheological Behavior of Magnetorheological Fluids: Step-Strain Experiments", *J. Smart Mater. Struct.* **11** 209–17

[9] Melek Yalcintas, 1995, "An Analytical and Experimental Investigation of Electrorheological Material Based Bdaptive Structures", *Dissertation Lehigh University.*

[10] Jalil Rezaeepazhand and Lotfollah Pahlavan, 2008, "Transient Response of Sandwich Beams with Electrorheological Core", *Journal of Intelligent Material Systems and Structures* 2009; 20; 171.